PCCP

Accepted Manuscript

ROYAL SOCIETY OF CHEMISTRY

www.rsc.org/pccp

Journal Name

RSCPublishing

ARTICLE

Energy transfer and spectroscopic characterization of perylenetetracarboxylic diimide (PDI) hexamer

Cite this: DOI: 10.1039/xoxxoooooox

Saran Long,[a] Yingying Wang,[a] Silvije Vdović,[a,b] Meng Zhou,[a] Linyin Yan,[a] Yingli Niu,[a] Qianjin Guo[a,*] and Andong Xia[a,*]

Received ooth January 2012,
Accepted ooth January 2012

DOI: 10.1039/xoxxoooooox

www.rsc.org/

We report a comprehensive study on a newly synthesized perylenetetracarboxylic diimide (PDI) hexamer together with its corresponding monomer and dimer by means of steady-state absorption and fluorescence as well as femtosecond broadband transient absorption measurements. The structure of PDI hexamer is nearly arranged in a 3-fold symmetry by three identical and separated dimers. This unique structure makes the excited state energy relaxation processes more complex due to the existence of two different intramolecular interactions: strong interaction between face-to-face PDIs in dimer, and relatively weak interaction among the three separated PDI dimers. The steady-state spectra and ground state structural optimization show that the steric effect plays dominant role in keeping the formation of the face-to-face stacked PDI-dimer within PDI-hexamer, indicating that there is some level of pre-associated excimer formed already in the ground state for dimer in hexamer. Femtosecond transient absorption experiments on PDI hexamer reveal a fast (~200 fs) localization process, and sequential relaxation to pre-associated excimer trap state from the delocalized exciton state with about 1.2 ps after initially delocalized excitation. Meanwhile, excitation energy transfer among the three separated dimers within PDI-hexamer is also revealed by the anisotropic femtosecond pump-probe transient experiments, where the hopping time is about 2.8 ps. A relaxed excimer state is further formed in 7.9 ps after energy hopping and conformational relaxation.

Introduction

Photosynthesis, which converts solar energy to chemical energy, is one of the most efficient biological processes in nature, where in the LH1 and LH2 bacterial photosynthetic antenna, the pigments are generally deliberately positioned in a wheel-like arrangement. To simulate efficient biological processes, the artificial light-harvesting functionality in assemble structures have been studied with the goal of applying these molecular arrays to molecular photonic devices or artificial light-harvesting systems. These studies revealed a fascinating interplay between photoexcitation localization/delocalization patterns and their energy-relaxation dynamics. For these reasons, it is important to understand excitation energy transfer process in both natural and artificial light harvesting systems as well as in materials for organic photovoltaics.[1] Supramolecular organic assemblies have attracted widespread interests due to the important position of the aggregated chlorophyll molecules inside purple bacteria in photosynthetic energy transfer[2-4], and numerous potential application in semiconductors in electronic devices[5-8] and functional materials in photovoltaic devices[9-11]. The self-assembly of the organic chromophores provide novel ideas and starting points to design and synthesize the rigid molecular as model systems by smaller chromophores.

In this paper, a newly synthesized perylenetetracarboxylic diimides (PDI) hexamer is used as an model for the study of the photophysical interactions within the face-to-face PDI pair and/or among the three identical PDI-dimers.[12] The molecular structure of PDI-hexamer is shown in Scheme 1. For comparison, the molecular structures of PDI-monomer and PDI-dimer are also shown in Scheme 1. PDIs have been thoroughly studied in the last few years as an active material for light harvesting,[13-17] photovoltaic applications,[16,18,19] and as model chromophores exhibiting basic photoinduced charge and energy transfer processes, whose main characteristics are outstanding photostability and the ability to self-assemble in solution, mostly by π-π stacking. In PDI-hexamer, as described in ref. 12, the six PDI units are nearly arranged in a 3-fold symmetry by three identical and separating face-to-face PDI dimers connected through central benzene ring. It is expected that two kinds of intermolecular interactions may exist: the strong coupling interaction within a face-to-face chromophore pair linked by the same N atom as a dimer, and the weak interaction among the three separated dimers. We investigate here the excited state kinetics of the mutibranched PDI hexamer using femtosecond pump-probe experiments combined with the steady-state spectroscopic measurements. By comparing the responses observed in monomer, dimer and hexamer, we are able to demonstrate the decay pathways associated with

chromophore-chromophore interactions in hexamer. The result is explained in terms of exciton-excimer model. Quantum chemical calculations suggest that the ground state dipole moments of two PDI chromophores in each dimer branch of hexamer are nearly parallel because of the steric effects; whereas the two PDI chromophores in free dimer are distant from each other because of the flexible linker. Furthermore, the spectral properties of free PDI-dimer behave more like two independent (or weak-coupled) monomers. Relative to that of the corresponding monomer and dimer, the fact that the steady-state absorption spectra of PDI-hexamer exhibit intensity redistribution with increased blue absorption and broad red-shifted emission spectra of PDI-hexamer, which is predicted by modified H-type exciton model, indicates the formation of a pre-associated excimer in ground state because of steric effects for dimer within hexamer. In femtosecond transient absorption for PDI-hexamer, exciton localization process is observed, which sequentially relaxes to the pre-associated excimer trap state. Polarization selective transient absorption shows the energy transfer among the three dimers within hexamer. All these results could be helpful in improving our knowledge on the structure-dependent optical properties of these compounds, enabling the design and synthesis of new chromophores with excellent optical properties.

Scheme 1. Molecular structures of PDI-hexamer, PDI-dimer and PDI-monomer.

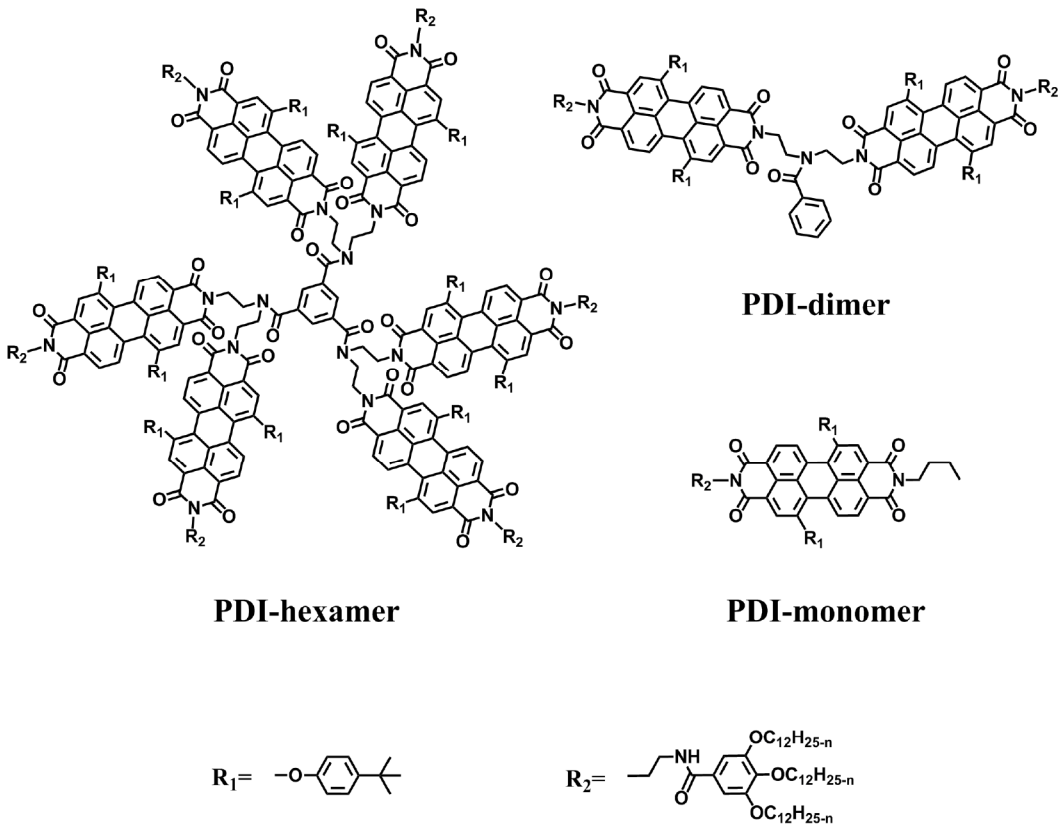

Experimental Methods

Steady-State Spectroscopy

The synthesis of PDI-monomer, PDI-dimer and PDI-hexamer has been described previously.[12] UV-vis absorption spectra were recorded with a U-3010 spectrophotometer (Hitachi, Japan). Corrected fluorescence and excitation spectra were obtained with a F-4600 fluorescence spectrometer (Hitachi, Japan) using a Xe lamp as the excitation source. All the experiments were carried out at room temperature.

Time Correlated Single Photon Counting (TCSPC) measurements

The time-resolved fluorescence lifetime measurements were carried out using a time-correlated single-photon counting (TCSPC) spectrometer (F900, Edinburgh, UK). The samples were excited at 500 nm using a picosecond LED source (PLS-500, PicoQuant, Germany). The instrument response function (IRF) of the detection is about 400 ps.

Femtosecond Transient Absorption Measurements

The transient absorption measurements with 90 fs time-resolution were measured using homemade femtosecond broadband pump-probe setup, which has been described in detail elsewhere.[20,21] Briefly, a regeneratively amplified Ti:sapphire laser (Coherent Legend Elite) produces 40 fs, 1 mJ pulses at a 500 Hz repetition rate with a spectrum centered at 800 nm and a bandwidth of 40 nm (FWHM). The output from the amplifier is split by a 90/10 beamsplitter into pump and probe beams. A portion of the 800-nm fundamental light was doubled in a 0.5 mm thick BBO (type I) crystal to provide the 400 nm pump pulse. For pumping at 520 nm, a TOPAS-C (Light Conversion, Lithuania) was used with pulse width of about 90 fs. About 100 nJ/pulse at 400 nm and 90 nJ/pulse at 520 nm used for excitations are focused into sample with 120

μm spot. A synchronized optical chopper (New Focus Model 3501) with a frequency of 250 Hz is inserted into the pump beam path in order to record spectra that are classified as pumped and not-pumped spectra, thereby reducing background. Every spectrum is recorded 360 times and the averaged spectrum is used in further data processing. The probe beam at 800 nm is sent to a variable optical delay line with maximal delay down to 1 ns, which comprises of a retro-reflector mirror on a computer controlled precision translation stage with a temporal resolution of 1 fs. The probe beam is then focused on a 2-mm-thick water cell to generate a white light continuum (WLC). The WLC provides a usable probe source between 430 and 780 nm selected by a bandpass filter. The WLC was then split into two beams using a broadband 50/50 beamsplitter for reference and signal beams. The signal beam is focused into a flow cell with 1 mm path length and spatially and temporally overlapped with the pump beam in the liquid sample, while the reference beam is passed through the unexcited volume of the sample. Both reference and signal beams after the sample are focused into optical fibers of a dual-channel spectrometer (Avantes AvaSpec-2048-2-USB2) triggered from the same synchronized optical chopper driver at 500 Hz. In isotropic transient absorption measurements the mutual polarization of pump and probe beams was set to the magic angle (54.7º). Using the two-beam method, a few algorithms of data acquisition can be applied with the most common being a relative normalization of the spectral intensity of the probe to the spectral intensity of the reference. For each pump pulse, spectral intensities of the signal and the reference without any excitation in the sample, I_{signal}^{off} and I_{ref}^{off}, respectively, and I_{signal}^{on} and I_{ref}^{on} in the presence of the pump, were measured. Then the ΔOD of the transient absorption (for a given time delay) can be calculated from the following formula:

$$\Delta \mathrm{OD}(t,\lambda) = -\log\left(\frac{I_{signal}^{on}(t,\lambda)}{I_{signal}^{off}(t,\lambda)} \times \frac{I_{ref}^{off}(t,\lambda)}{I_{ref}^{on}(t,\lambda)}\right) \qquad (1)$$

Data Analysis

Before global fitting, a wavelength-dependent time-zero correction was performed to account for the group velocity dispersion of the probe beam using a commercial fitting software (FemtoSuite, IB Photonics Ltd.). The differential absorbance $\Delta A(t,\lambda)$ was analyzed using the population dynamics modeling graphical interface program Glotaran and TIMP,[22] where a sequential model was used to model the $\Delta A(t,\lambda)$ data. The transient absorption spectra are globally fitted with the sequential model and the associated spectra are called evolution associated difference spectra (EADS), which can be described as

$$\Delta A(t,\lambda) = \sum_{i=1}^{n} c_i^{EADS}(t)\, EADS_i(\lambda) \qquad (2)$$

with $c_i^{EADS}(t) = \sum_{j=1}^{i} b_{ji} \exp(-kjt) \oplus i(t)$ and $b_{ji} = \prod_{m=1}^{i} k_m \Big/ \prod_{n=1,n\neq j}^{i} (k_n - k_j)$, where $i(t)$ is the instrument response function (IRF), k_j is the decay rate of component j and the amplitudes b_{ji} of the exponential decays are defined for $j \le i$ assuming $b_{11} = 1$. The EADS represents the spectral evolution with successively increasing lifetime.

The time-resolved anisotropic decay r(t) was calculated from the decay curves under the parallel polarizations $I_{\parallel}(t)$ and perpendicular polarizations $I_{\perp}(t)$ based on the tail matching correction according to equation (3):[23-25]

$$r(t) = \frac{I_{\parallel}(t) - I_{\perp}(t)}{I_{\parallel}(t) + 2I_{\perp}(t)} \qquad (3)$$

where $I_{\parallel}(t)$ and $I_{\perp}(t)$ represent signals with the polarizations of the pump and probe pulses being mutually parallel and perpendicular, respectively.

The 0.1 mM solution of sample in spectral grade chloroform was prepared under dim light and circulated in a flow cell with a path length of 1 mm to ensure that a fresh sample volume was exposed to each pump pulse. No photodegradation was observed after femtosecond transient absorption measurements.

Results and Discussion

Steady-State Spectroscopy

Figure 1a shows the steady-state absorption and fluorescence spectra of PDI-monomer, PDI-dimer and PDI-hexamer dissolved in chloroform. It is found that PDI-monomer shows an absorption maximum peak around 545 nm together with two lower intensity vibronic peaks around 510 and 470 nm corresponding to the strong allowed $S_0 \rightarrow S_1$ transition of PDI with the transition dipole moment oriented along the long axis of PDI molecule. A second peak around 400 nm and attributed to transition involving a higher excited state ($S_0 \rightarrow S_2$) with the transition dipole moment oriented along the short axis of PDI molecule, which is similar with other reported PDIs.[26,27] Meanwhile, the absorption of PDI-hexamer shows two red shifted maximum around 555 and 520 nm with a shoulder around 480 nm. Compared to PDI-monomer, a dramatic intensity change between the two main bands (555 and 520 nm) in PDI-hexamer is seen, where the intensity ratio of $I_{555\ nm}/I_{520\ nm}$ is about 1.04 for PDI-hexamer, and about 1.52 for PDI-monomer, respectively. According to Kasha's theory, there are two types of the exciton models (H- and J-type) to predict the observed spectral behaviors.[28] The coupling of two transition dipoles causes splitting of the lowest energy electronic transition into two exciton bands, with the higher energy band having all of the oscillator strength for H-type face-to-face stacking, whereas with the lower energy band having most of the oscillator strength for J-type arrangement.[28] This generates two bands, with the upper one being an allowed and intense absorption transition from the ground state for an H-type structure while the lower level is allowed for the absorption transition for the J-type model. Therefore, the dramatic decrease in the intensity ratio of $I_{555\ nm}/I_{520\ nm}$ of PDI-hexamer (~1.04) relative to that of PDI-monomer (~1.52) suggests the existence of the delocalized exciton states in PDI-hexamer, where an H-type aggregate is formed in PDI-hexamer.[12,29] This can be further confirmed from following ground state structural optimization.

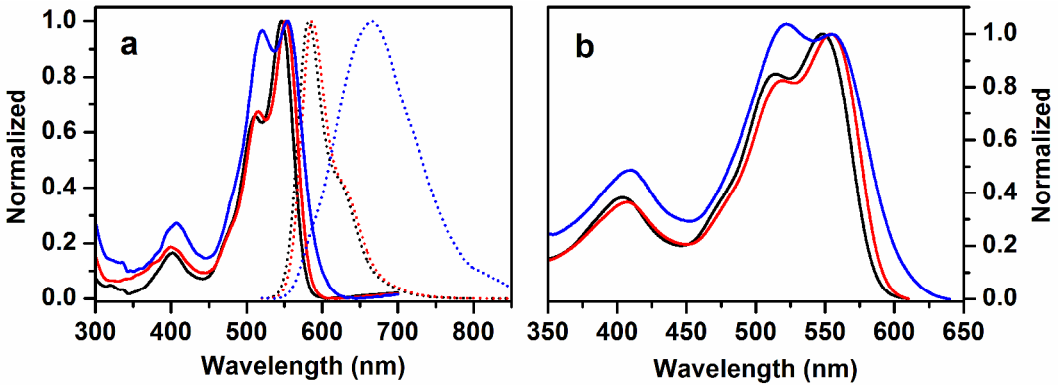

Figure 1. Normalized steady-state absorption (solid lines) and fluorescence (dotted lines) spectra of PDI-monomer (black), PDI-dimer (red) and PDI-hexamer (blue) measured in chloroform (a). The fluorescence excitation spectra were monitored at 630 nm for PDI-monomer (black) and PDI-dimer (red) and 660 nm for PDI-hexamer (blue) (b). The concentration of PDI-hexamer used here were low enough to ensure no intermolecular self-assembled structures exist.[12] (see Figure S1, ESI†)

In order to check the alignment of transition dipoles of the PDI molecules in hexamer, we performed ground state structural optimization with AM1 model as implemented in the Gaussian 03 software package.[30] Solvation effect is neglected during optimization. The optimized ground state geometries of PDI-hexamer is displayed in Scheme 2. The optimized results show six PDIs linked via C-N bonds on the benzene ring. Each pair of PDIs linked by the same N atom is regarded as a dimer branch, where the three dimers exhibit C_3-symmetry. The center-to-center distance between the two PDIs in one dimer is about 8 Å, while the distance between two adjacent dimers is longer than 15 Å. It is found that the hydrogen bond exists between the amide nitrogen and carbonyl oxygen in one dimer, and a slight distortion of the aromatic core is caused by the presence of the butylphenoxy substituents in the bay regions. Their aggregation modes determined by Li using XRD analysis and MM+ calculations confirmed the optimized structure here.[12] In addition, each PDI chromophore in one branch dimer is close to a cofacial structure, with the rotational displacement angle between the two coupled PDI planes about 38º. Since transition dipole of PDI is oriented along the long N-N axes, the transition dipoles in each coupled PDI-dimer are not strictly parallel to each other. Therefore, according to the adjusted zero-order exciton theory, the molecular vibration coupled strongly with electronic transitions could slightly change the selection rules, and transitions from the ground state to both exciton levels are allowed.[31-33]

Scheme 2. Energy-minimized ground state structure of PDI-hexamer (a). The enlarged dimer part of PDI-hexamer (b).

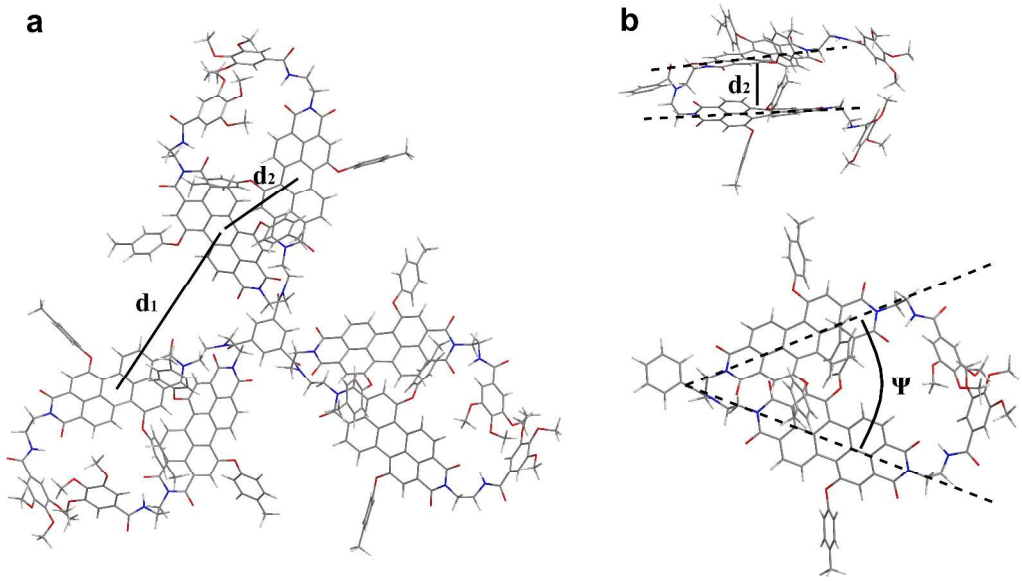

d_1 is the smallest center-to-center distance between the two PDIs in different dimers; d_2 is the center-to-center distance between the two PDIs in one dimer; Ψ is the rotational displacement angle.

As shown in Figure 1, the fluorescence excitation spectrum of PDI-monomer is nearly the same as the absorption spectrum for PDI-monomer, but that is significantly different for PDI-hexamer, where the intensity of 520 nm peak becomes stronger

than that of 555 nm peak, in line with the H-type dimer model. It is possible that the interactions among these three H-type dimers in PDI-hexamer may further slightly adjust the energy levels to form the low-energy excimer state, even though the coupling among these three dimers is much weaker because of the long distance. Furthermore, the intensities of 520 nm excitation peaks of PDI-hexamer gradually increase (see fluorescence excitation spectra in Figure S2, ESI†), when monitored emission wavelength changes from 600 to 730 nm, further indicating the formation of excimer state dominated in long wavelength region. The fluorescence spectra of PDI-monomer and -hexamer as shown in Figure 1a are significantly different. PDI-monomer has a sharp, well-resolved fluorescence spectrum, relative small Stokes shift with an emission maximum around 580 nm and a vibronic band around 625 nm (typical mirror image of the absorption band). On the other hand, fluorescence spectrum of PDI-hexamer shows a broad and featureless with a largely red-shifted maximum around 665 nm. Moreover, the fluorescence lifetime of PDI-monomer is about 4.8 ns (see Figure S3, ESI†), whereas the lifetimes of PDI-hexamer show two typical values with a short one about 3.3 ns and a long one about 20 ns (see Figure S4, ESI†) The short lifetime (~3.3 ns) is corresponding to the interacted exciton states or monomer dominated at blue-side of emission spectra, and the long lifetime (~20 ns) mainly corresponds to the excimer state of PDI-hexamer. As shown in Table S1, the increasing pre-exponential factor of the long lifetime monitored at long emission wavelengths suggests the formation of typical low-energy excimer state in PDI-hexamer, which lies below the nearby lower-energy exciton state.

In addition, we also carefully compare the steady-state spectra and fluorescence lifetime results of free PDI-dimer with that of PDI-monomer and -hexamer, (see Figure 1 and Figure S2-S4, ESI†) and it is surprised that all of the spectral characteristics seen in PDI-dimer resembled the results obtained from PDI-monomer rather than PDI-hexamer. We believe that this is because the geometrical arrangement of two PDI units in free dimer is totally different from that in the dimer in hexamer, where the rotational displacement angle is much larger in dimer (Ψ = 119º) (see Figure S5a, ESI†) compared to that in hexamer (Ψ = 38º) (see Scheme 2b) because of steric effect. Therefore, in free dimer, two PDIs are distant from each other because of the flexible linker, and the spectra of free PDI-dimer behave more like two independent (or weak-coupled) monomers. This suggests that the steric effect plays dominant role in keeping the formation of the face-to-face stacked PDI-dimer within PDI-hexamer. In other words, as shown in Figure 1b and Figure S2 (ESI†), the non-overlap of the fluorescence excitation spectra of the free dimer and hexamer indicates that there is some level of pre-associated excimer formed already in the ground state because of steric effect for dimer in hexamer. Ground state cofacial stacking is known to promote excimer formation by greatly enhanced interaction of the initially localized excited state with one of the ground state molecule in the face-to-face PDIs.[34,35] Similar emission spectra have been observed previously in tethered PDI oligomers.[36-38] The low fluorescence quantum yield of hexamer less than 0.01,[12] and very long lifetime (up to ~20 ns) (see Figure S4, ESI†) are typical evidence of excimer formation, where the low concentration PDI-hexamer used for the experiments ensures the excimer formation is from the two closely packed PDIs in a dimer of hexamer.

Femtosecond Time-Resolved Transient Absorption

Figure 2 shows the femtosecond time-resolved transient absorption spectra at different delay times of PDI-monomer and PDI-hexamer in chloroform following 400 nm, 90 fs excitation, where those transient absorption spectra at longer delay times are shown in Figure S6 (ESI†). As shown in Figure 2a, photoexcitation to S_2 state of PDI-monomer results in ground state bleaching (GSB) seen as a negative band extending from 450 to 650 nm with two GSB peaks around 510 and 550 nm, accompanied by positive excited state absorption (ESA) band in the 650-780 nm range. This ESA band probably extends to GSB region in transient absorption spectra which is masked because of strong overlap with more pronounced GSB and stimulated emission (SE) bands. The GSB band corresponds well to the steady-state absorption spectra of PDI-monomer. Partially overlapped with the GSB band, a strong SE appears at wavelengths corresponding to the steady-state fluorescence (550-650 nm). All these features are in agreement with previously published results for similar PDI-monomers.[39-41] The transient absorption spectrum of PDI-hexamer seems similar with that of PDI-monomer, and features a negative GSB band (450-600 nm) and a positive ESA band (600-780 nm). A closer looking at the transient absorption spectrum of PDI-hexamer relative to that of PDI-monomer reveals that the ESA band in hexamer shows time dependent blue/red-shift and broadening, indicating a typical characteristic of the formation of excimer state.[37,42] The SE band in the 550-650 nm range observed in monomer is invisible in hexamer due to formation of the excimer state with a very low fluorescence quantum yield.

To extract the excited state relaxation dynamics of PDI-monomer and PDI-hexamer, a suitable kinetic model was then necessary to fit the data shown in Figure 2. For PDI-monomer, the excitation at 400 nm directly populates the S_2 state, and then the excited monomer relaxes to the S_1^{vib} state via internal conversion, and sequentially vibrational cooling to the lowest vibrational level of S_1, which is common in PDI or other molecules in previous reports[41,43,44], therefore a sequential kinetic model is quite suitable for the global analysis of PDI-monomer. For PDI-hexamer, as mentioned above from steady-state spectral properties and ground state structural optimization, there are three separated face-to-face cofacial stacking dimers in hexamer, and a broad and largely red-shifted structureless fluorescence spectrum with long lifetime (up to 20 ns) was observed, suggesting the formation of a low-energy excimer state. This is the typical feature of the excimer's emission from the face-to-face stacked PDI-dimer (H-type).[12,35] Because the lower exciton band of the dimer is forbidden with less intense absorption transition from the ground state for an H-type structure, that as mentioned above, a low energy pre-associated excimer already exist below the lower-energy exciton state, where the relaxation from exciton state to the pre-associated excimer is very fast less than 4.5 ps or even more faster as reported previously,[36,45] and after an excitation, the excited state relaxation in the face-to-face dimer (H-type) will play a main role in excited PDI-hexamer,[42,45,46] while a sequential kinetic model is also appropriate for the global analysis of the time-resolved data of PDI-hexamer as predicted from Kasha model.[28] Although, the free dimer (see Figure S5) is not an ideal model for making comparison with the dimer in hexamer, several PDI-dimers with the similar face-to-face π-stacking geometry as the PDI-dimer in our PDI-hexamer have been reported,[17,38,45,46] where the spectral features and excited state dynamics observed in our PDI-hexamer are very similar to the behaviours observed in those reported PDI-dimers.

Therefore, together with the conclusion from the steady-state measurements, the sequential scheme could be used for modeling the transient data of both monomer and hexamer, that is, EADS associated with certain kinetic profile represents the spectral features following that dynamics, the corresponding time constant can be regarded as the lifetime of each EADS.[47]

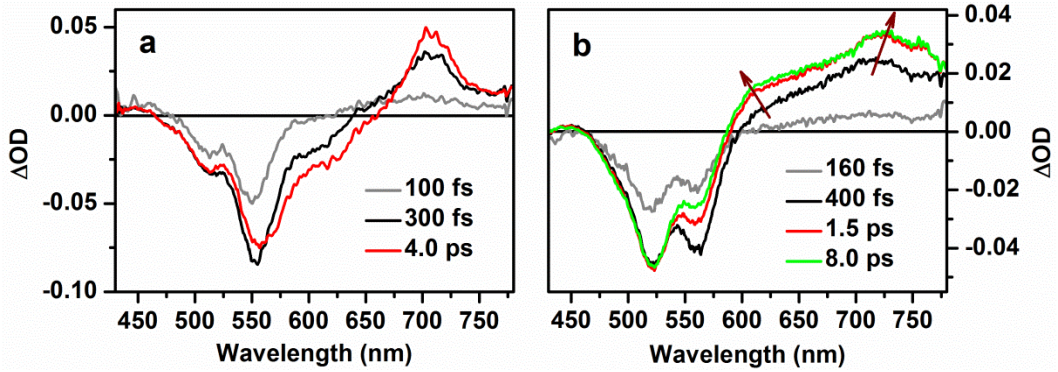

Figure 2. Femtosecond transient absorption spectra for PDI-monomer (a) and PDI-hexamer (b) in chloroform following excitation at 400 nm. Arrows in (b) reflect the ESA peaks blue/red shifted with time delay.

Sequential kinetic models used in the global analysis of the time-resolved data and resulting EADS for PDI-monomer and PDI-hexamer are shown in Figure 3. The fitted time constants are also listed in Table S2 (ESI†). For monomer, two major components are required to obtain the best fitting. The internal conversion process from S_2 state to S_1^{vib} state after excitation is less than 100 fs that beyond the resolution of the detection. The first component with time constant of about 3.6 ps (red line in Figure 3c) corresponds to vibrational relaxation from S_1^{vib} to the lowest vibrational level of S_1. This EADS has an ESA band between 650 and 780 nm, which can be ascribed to the S_1^{vib} state. The second component (blue line in Figure 3c) is associated with the decay of S_1 state to the ground state with a decay time constant of about 2.5 ns, in line with fluorescence lifetime of PDI-monomer obtained from time correlated single photon counting (TCSPC) measurements. The GSB recovery at 550 nm of this EADS is mainly attributed to the superposition of the negative GSB band with the positive ESA together with the negative SE band. Kühn and his coworkers had investigated a PDI chromophore whose molecular structure resembled the structure of the PDI-monomer, excepted for having four substituents at bay positions.[26] Their calculated ESA spectrum shows two broad features, one between 500 and 600 nm and another one extending from 650 to 750 nm.[26] It is reasonable to expect that the GSB peak at 550 nm is influenced by ESA more heavily than that at 510 nm. Meanwhile, For PDI hexamer, three components are needed to obtain the best fitting of the pump-probe data of PDI-hexamer. The ultrafast time constants of the decay process from S_2 to the exciton states and the internal conversion between the two exciton states could not be resolved because of the limited time-resolution. The EADS of first component (red line in Figure 3d) represents the exciton equilibration and localization with a lifetime of 1.2 ps, indicating that the energy relaxation from the exciton states to the pre-associated excimer state evolves on a 1.2 ps lifetime. The second EADS (green line in Figure 3d) contains a more intense GSB peak at 520 nm than at 560 nm similar to the shape of the fluorescence excitation spectrum of hexamer (as shown in Figure 1b) and a slightly blue/red-detuned ESA (as indicated with arrows in Figure 2b) in the region of 600-780 nm which further proves the formation of excimer state.[37,42] Recently, Wasielewski and coworkers had investigated the energy flow dynamics and the excimer formation of cofacial PDI dimers.[45,46,48] They mentioned an 8-17 ps relaxation in the model which is assigned to geometric rearrangement from the initial unrelaxed excimer state to a more relaxed excimer conformation due to the existence of the displacement rotational angle between the long N-N axsis.[45] In our case, the PDI hexamer has a similar conformation (as shown in Scheme 2) so that the 7.9 ps component is attributed to the relaxation from the unrelaxed to a more relaxed excimer state. That is, in the hexamer it takes about 7.9 ps for dimer to reach the relaxed excimer geometry, which is expected to have the long N-N axes of the two PDIs parallel to each other, since the rotational displacement angle between the two PDI planes is about 38°.[45,49] The formation of relaxed excimer is so fast (~7.9 ps), and this is why there is no evidence for a rise time at 680 nm observed from TCSPC experiments (see Figure S4 and Table S1, ESI†) because the limited time resolution of TCSPC measurements. The third EADS (blue line in Figure 3d) corresponds to the decay process from the relaxed excimer state to the ground state with a very long lifetime up to 20 ns obtained from the fitting, which is in accordance with the TCSPC result.

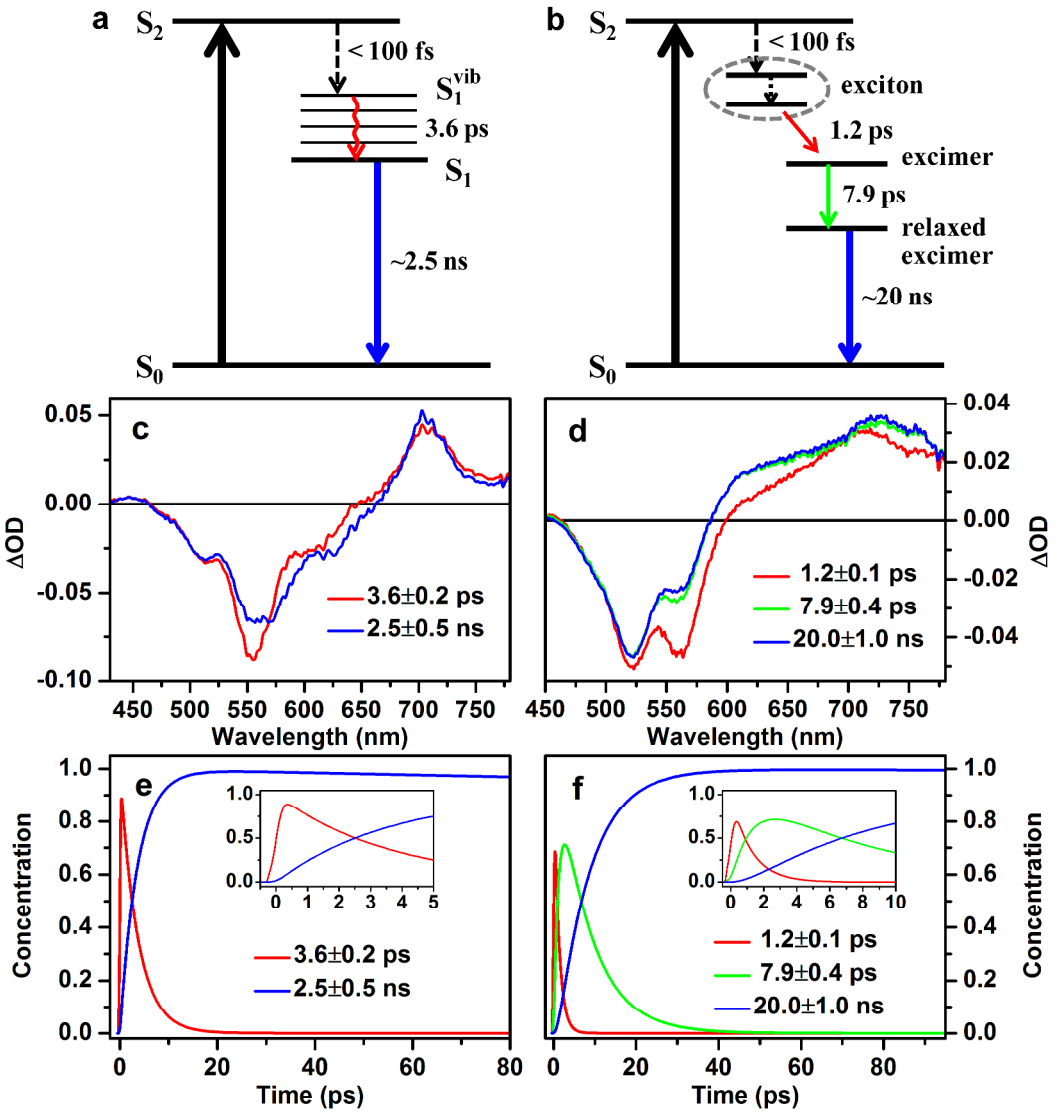

Figure 3. Sequential reaction scheme for PDI-monomer (a) and PDI-hexamer (b), respectively, showing the relaxation pathways after excitation with 400 nm. EADS of monomer (c) and hexamer (d) fitted with the corresponding sequential models. The associated population evolution curves of the EADS components for monomer (e) and hexamer (f). Insets show the initial stages of evolutions of excited stated relaxation. Kinetics at selected single wavelengths for showing the quality of global fitting for PDI-monomer and -hexamer are shown in Figure S7 and S9 (ESI†), respectively.

It should be mentioned that photoinduced electron-transfer is another important photophysical process usually considered in PDI-related chromophores and aggregates.[42,50,51] Numerous previous studies found that charge transfer can occur in the case of stronger electron donating bay-substituents such as triphenylamine,[40] for example, the electron transfer from the 3,4,5-tridodecyloxyphenyl at the imide N atoms substituents to the two phenoxy substituents in PDI core was reported, which leads to the nonemissive charge-separated excited states.[52] Since photoinduced charge transfer process may be initiated in our systems, the red-shifted peak around 730 nm in the transient absorption spectrum could be assigned to PDI^- ion in the transient absorption spectrum.[42,50,53] However, it is more probable that the formation of excimer dominates in the energy relaxation of PDI hexamer.

As mentioned above, PDI-hexamer composed of six PDI monomers results in two kinds of interactions among/between these PDI chromophores. We believe that a strong excitonic interaction exists between the two chromophores in one dimer, and an electronic energy transfer hopping occurs among these three dimers. To further explore the relaxation dynamics of the excited-state interaction, we performed the anisotropic femtosecond transient absorption experiments. The anisotropy change implies a dependence on the relative orientation between pump and probe polarization which is caused by reorientation of excitonically coupled transition dipole moments or by differently oriented transition dipole moments when energy hopping process occurs.[44,54,55] Figure 4 presents the time dependence of the anisotropy of monomer and hexamer both probed at 560 nm following 520 nm excitation. For monomer, it is found that there is no obvious anisotropy decay within the time period of measurement with a high initial r(0) around 0.35, indicating slow rotation of monomer molecule. On the contrary, the hexamer shows fast 200 fs depolarization, and the value of anisotropy decreases from near 0.4 to 0.1 during this fast initial decay. It then reduces further to 0.03 on a

2.8 ps time scale. These features indicate complex relaxation dynamics in PDI-hexamer determined by energy transfer from the exciton to excimer state. Combined with the isotropic transient absorption results, the fast 200 fs component of the anisotropy decay in hexamer reflect the strong interaction between the PDIs, where the intial delocalized exciton state formed over a substantial portion of the hexamer is subsequently localized on one branch, leading to the initial fast depolarization, which is in accordance with the exciton localization time scale obtained from isotropic transient absorption. The slower 2.8 ps decay component reflects incoherent hopping among the three dimer-branches followed by the formation of the relaxed excimer state. This behavior is usually seen in multi-branched macromolecules and photosynthetic light-harvesting antenna pigment systems, within the similar time scale as estimated using Förster energy transfer theory.[56]

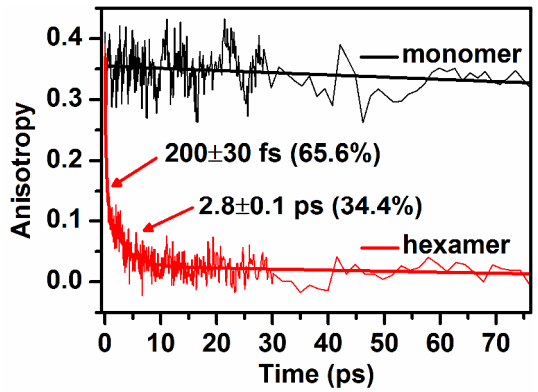

Figure 4. Femtosecond transient absorption anisotropy decays of monomer and hexamer probed at 560 nm following 520 nm excitation. Fitting results are also shown.

Comparing the results obtained from isotropic and anisotropic transient absorption measurements, it is found that the fast anisotropy changes resulted from the exciton interaction and energy-migration processes, occurring simultaneously with the exciton localization on one site observed in isotropic data within the similar time scale. Obviously, initially delocalized symmetrical excited state is also affected by some energy dissipation processes like solvation and vibrational relaxation, which introduce dynamic disorder, leading to the accelerated localization of the excitation.[57] However, the detailed analysis of these processes is beyond the scope of this paper because of the limited time-resolution.

Conclusions

In summary, a mutibranched PDI hexamer was investigated by employing both steady-state and femtosecond transient absorption measurements in order to gain deeper insight into the energy flow mechanism. Comparative study of PDI-hexamer and corresponding PDI-monomer and PDI-dimer chromophores is helpful in developing the following energy transfer scenario based on exciton-excimer model in PDI-hexamer. That is, upon an ultrafast excitation, the delocalized excited states are initially presented in PDI-hexamer, while exciton dephasing and exciton localization occur on a ~200 fs ultrafast time scale with the excitation energy localized on one site chromophore because of the structural disorder. Subsequently the energy are relaxed to the lower energy pre-associated excimer state within 1.2 ps, followed by the formation of the relaxed excimer state in 7.9 ps time scale. Simultaneously, the energy migration (hopping) among the three coupled dimers with time constant of about 2.8 ps is observed. We expect this phenomenon to be quite general and not restricted to specific molecular structures. Our results provide structural insights for the excited state relaxation of aggregates of PDI derivatives.

Acknowledgements

A. X. thanks Prof. Xiyou Li from Shandong University for providing PDI-monomer, -dimer, and -hexamer samples. S. V. thanks the support by CAS Research Fellowship for International Young Researchers. This work was supported by the 973 Program (2013CB834604), NSFCs (21173235, 91233107, 21127003, 21333012 and 21373232) and the Strategic Priority Research Program of the Chinese Academy of Sciences (Grant No. XDB12020200).

Notes and references

[a] Beijing National Laboratory for Molecular Sciences (BNLMS), Institute of Chemistry, Chinese Academy of Sciences, Beijing 100190, People's Republic of China. E-mail: andong@iccas.ac.cn, guoqj@iccas.ac.cn.
[b] Institute of Physics, Bijenička cesta 46, 10000 Zagreb, Croatia.

† Electronic Supplementary Information (ESI) available: Flurescence excitation spectra monitored at different emission wavelengths and fluorescence lifetime measurements by TCSPC of PDI-monomer, -dimer and -hexamer; Energy-minimized structure and transient absorption results of free PDI-dimer. See DOI: 10.1039/b000000x/

1 M. R. Wasielewski, *Acc. Chem. Res.*, 2009, **42**, 1910-1921.
2 D. Kim and A. Osuka, *Acc. Chem. Res.*, 2004, **37**, 735-745.
3 A. Huijser, T. J. Savenije, A. Kotlewski, S. J. Picken and L. D. A. Siebbeles, *Adv. Mater.*, 2006, **18**, 2234-2239.
4 X. Li, L. E. Sinks, B. Rybtchinski and M. R. Wasielewski, *J. Am. Chem. Soc.*, 2004, **126**, 10810-10811.
5 J. Stangl, V. Holý and G. Bauer, *Rev. Mod. Phys.*, 2004, **76**, 725-783.
6 H. Hlaing, X. Lu, T. Hofmann, K. G. Yager, C. T. Black and B. M. Ocko, *ACS Nano*, 2011, **5**, 7532-7538.
7 G. R. Dholakia, W. Fan, J. Koehne, J. Han and M. Meyyappan, *Phys. Rev. B*, 2004, **69**, 153402.
8 L. Wong, C. Hu, R. Paradise, Z. Zhu, A. Shtukenberg and B. Kahr, *J. Am. Chem. Soc.*, 2012, **134**, 12245-12251.
9 P. V. Kamat, *J. Phys. Chem. C*, 2007, **111**, 2834-2860.
10 J. Peet, A. J. Heeger and G. C. Bazan, *Acc. Chem. Res.*, 2009, **42**, 1700-1708.
11 D. Dalacu, M. E. Reimer, S. Fréderick, D. Kim, J. Lapointe, P. J. Poole, G. C. Aers, R. L. Williams, W. Ross McKinnon, M. Korkusinski and P. Hawrylak, *Laser Photonics Rev.*, 2010, **4**, 283-299.
12 L. Xue, H. Wu, Y. Shi, H. Liu, Y. Chen and X. Li, *Soft Matter*, 2011, **7**, 6213-6221.
13 S. Prathapan, S. I. Yang, J. Seth, M. A. Miller, D. F. Bocian, D. Holten and J. S. Lindsey, *J. Phys. Chem. B*, 2001, **105**, 8237-8248.
14 S. I. Yang, S. Prathapan, M. A. Miller, J. Seth, D. F. Bocian, J. S. Lindsey and D. Holten, *J. Phys. Chem. B*, 2001, **105**, 8249-8258.
15 K.-y. Tomizaki, R. S. Loewe, C. Kirmaier, J. K. Schwartz, J. L. Retsek, D. F. Bocian, D. Holten and J. S. Lindsey, *J. Org. Chem.*, 2002, **67**, 6519-6534.

16 Z. Chen, V. Stepanenko, V. Dehm, P. Prins, L. D. A. Siebbeles, J. Seibt, P. Marquetand, V. Engel and F. Würthner, *Chem. Eur. J.*, 2007, **13**, 436-449.
17 L. Xue, Y. Shi, L. Zhang and X. Li, *ChemPhysChem*, 2013, **14**, 3319-3326.
18 S.-G. Chen, P. Stradins and B. A. Gregg, *J. Phys. Chem. B*, 2005, **109**, 13451-13460.
19 B. A. Gregg and R. A. Cormier, *J. Am. Chem. Soc.*, 2001, **123**, 7959-7960.
20 M. Zhou, S. Vdović, S. Long, M. Zhu, L. Yan, Y. Wang, Y. Niu, X. Wang, Q. Guo, R. Jin and A. Xia, *J. Phys. Chem. A*, 2013, **117**, 10294-10303.
21 S. Jin, S. Wang, Y. Song, M. Zhou, J. Zhong, J. Zhang, A. Xia, Y. Pei, M. Chen, P. Li and M. Zhu, *J. Am. Chem. Soc.*, 2014, **136**, 15559-15565.
22 J. J. Snellenburg, S. P. Laptenok, R. Seger, K. M. Mullen and I. H. M. van Stokkum, *J. Stat. Software*, 2012, **49**, 1-22.
23 M. Sajadi, M. Weinberger, H.-A. Wagenknecht and N. P. Ernsting, *Phys. Chem. Chem. Phys.*, 2011, **13**, 17768-17774.
24 J. R. Lakowicz, I. Gryczynski, H. Malak and Z. Gryczynski, *J. Phys. Chem.*, 1996, **100**, 19406-19411.
25 K.-S. Chang, L. Luo, C.-W. Chang, Y.-C. Huang, C.-Y. Cheng, C.-S. Hung, E. W.-G. Diau and Y.-K. Li, *J. Phys. Chem. B*, 2010, **114**, 4327-4334.
26 D. Ambrosek, H. Marciniak, S. Lochbrunner, J. Tatchen, X.-Q. Li, F. Würthner and O. Kühn, *Phys. Chem. Chem. Phys.*, 2011, **13**, 17649-17657.
27 Y. Chen, L. Chen, G. Qi, H. Wu, Y. Zhang, L. Xue, P. Zhu, P. Ma and X. Li, *Langmuir*, 2010, **26**, 12473-12478.
28 M. Kasha, H. R. Rawls and M. A. El-Bayoumi, *Pure Appl. Chem.*, 1965, **11**, 371-392.
29 Z. Chen, U. Baumeister, C. Tschierske and F. Würthner, *Chem. Eur. J.*, 2007, **13**, 450-465.
30 M. J. Frisch, G. W. Trucks, H. B. Schlegel, G. E. Scuseria, M. A. Robb, J. R. Cheeseman, J. A. Montgomery, Jr., T. Vreven, K. N. Kudin, J. C. Burant, J. M. Millam, S. S. Iyengar, J. Tomasi, V. Barone, B. Mennucci, M. Cossi, G. Scalmani, N. Rega, G. A. Petersson, H. Nakatsuji, M. Hada, M. Ehara, K. Toyota, R. Fukuda, J. Hasegawa, M. Ishida, T. Nakajima, Y. Honda, O. Kitao, H. Nakai, M. Klene, X. Li, J. E. Knox, H. P. Hratchian, J. B. Cross, V. Bakken, C. Adamo, J. Jaramillo, R. Gomperts, R. E. Stratmann, O. Yazyev, A. J. Austin, R. Cammi, C. Pomelli, J. W. Ochterski, P. Y. Ayala, K. Morokuma, G. A. Voth, P. Salvador, J. J. Dannenberg, V. G. Zakrzewski, S. Dapprich, A. D. Daniels, M. C. Strain, O. Farkas, D. K. Malick, A. D. Rabuck, K. Raghavachari, J. B. Foresman, J. V. Ortiz, Q. Cui, A. G. Baboul, S. Clifford, J. Cioslowski, B. B. Stefanov, G. Liu, A. Liashenko, P. Piskorz, I. Komaromi, R. L. Martin, D. J. Fox, T. Keith, M. A. Al-Laham, C. Y. Peng, A. Nanayakkara, M. Challacombe, P. M. W. Gill, B. Johnson, W. Chen, M. W. Wong, C. Gonzalez and J. A. Pople, GAUSSIAN 3 (Revision E.01), Gaussian Inc., Wallingford, CT, 2004.
31 R. L. Fulton and M. Gouterman, *J. Chem. Phys.*, 1964, **41**, 2280-2286.
32 J. Seibt, P. Marquetand, V. Engel, Z. Chen, V. Dehm and F. Würthner, *Chem. Phys.*, 2006, **328**, 354-362.
33 A. E. Clark, C. Qin and A. D. Q. Li, *J. Am. Chem. Soc.*, 2007, **129**, 7586-7595.
34 H. Saigusa and E. C. Lim, *Acc. Chem. Res.*, 1996, **29**, 171-178.
35 Y. Wang, Y. Chen, R. Li, S. Wang, W. Su, P. Ma, M. R. Wasielewski, X. Li and J. Jiang, *Langmuir*, 2007, **23**, 5836-5842.
36 Y. Wang, H. Chen, H. Wu, X. Li and Y. Weng, *J. Am. Chem. Soc.*, 2009, **131**, 30-31.
37 J. M. Giaimo, J. V. Lockard, L. E. Sinks, A. M. Scott, T. M. Wilson and M. R. Wasielewski, *J. Phys. Chem. A*, 2008, **112**, 2322-2330.
38 H. Yoo, J. Yang, A. Yousef, M. R. Wasielewski and D. Kim, *J. Am. Chem. Soc.*, 2010, **132**, 3939-3944.
39 E. Fron, R. Pilot, G. Schweitzer, J. Qu, A. Herrmann, K. Müllen, J. Hofkens, M. Van der Auweraer and F. C. De Schryver, *Photochem. Photobiol. Sci.*, 2008, **7**, 597-604.
40 E. Fron, G. Schweitzer, P. Osswald, F. Würthner, P. Marsal, D. Beljonne, K. Müllen, F. C. De Schryver and M. Van der Auweraer, *Photochem. Photobiol. Sci.*, 2008, **7**, 1509-1521.
41 J. M. Lim, P. Kim, M.-C. Yoon, J. Sung, V. Dehm, Z. Chen, F. Würthner and D. Kim, *Chem. Sci.*, 2013, **4**, 388-397.
42 B. Rybtchinski, L. E. Sinks and M. R. Wasielewski, *J. Phys. Chem. A*, 2004, **108**, 7497-7505.
43 M. Kullmann, A. Hipke, P. Nuernberger, T. Bruhn, D. C. G. Götz, M. Sekita, D. M. Guldi, G. Bringmann and T. Brixner, *Phys. Chem. Chem. Phys.*, 2012, **14**, 8038-8050.
44 H. S. Cho, H. Rhee, J. K. Song, C.-K. Min, M. Takase, N. Aratani, S. Cho, A. Osuka, T. Joo and D. Kim, *J. Am. Chem. Soc.*, 2003, **125**, 5849-5860.
45 R. J. Lindquist, K. M. Lefler, K. E. Brown, S. M. Dyar, E. A. Margulies, R. M. Young and M. R. Wasielewski, *J. Am. Chem. Soc.*, 2014, **136**, 14912-14923.
46 E. A. Margulies, L. E. Shoer, S. W. Eaton and M. R. Wasielewski, *Phys. Chem. Chem. Phys.*, 2014, **16**, 23735-23742.
47 I. H. M. van Stokkum, D. S. Larsen and R. van Grondelle, *Biochim. Biophys. Acta*, 2004, **1657**, 82-104.
48 K. E. Brown, W. A. Salamant, L. E. Shoer, R. M. Young and M. R. Wasielewski, *J. Phys. Chem. Lett.*, 2014, **5**, 2588-2593.
49 A. Schubert, V. Settels, W. Liu, F. Würthner, C. Meier, R. F. Fink, S. Schindlbeck, S. Lochbrunner, B. Engels and V. Engel, *J. Phys. Chem. Lett.*, 2013, **4**, 792-796.
50 B. Rybtchinski, L. E. Sinks and M. R. Wasielewski, *J. Am. Chem. Soc.*, 2004, **126**, 12268-12269.
51 T. Kircher and H.-G. Löhmannsröben, *Phys. Chem. Chem. Phys.*, 1999, **1**, 3987-3992.
52 F. Würthner, C. Thalacker, S. Diele and C. Tschierske, *Chem. Eur. J.*, 2001, **7**, 2245-2253.
53 H. Khandelwal, A. R. Mallia, R. T. Cheriya and M. Hariharan, *Phys. Chem. Chem. Phys.*, 2012, **14**, 15282-15285.
54 Y. Nakamura, I.-W. Hwang, N. Aratani, T. K. Ahn, D. M. Ko, A. Takagi, T. Kawai, T. Matsumoto, D. Kim and A. Osuka, *J. Am. Chem. Soc.*, 2005, **127**, 236-246.
55 F. Schlosser, J. Sung, P. Kim, D. Kim and F. Würthner, *Chem. Sci.*, 2012, **3**, 2778-2785.
56 F. Zhao, X. Zheng, J. Zhang, H. Wang, Z. Yu, J. Zhao and L. Jiang, *J. Photochem. Photobiol. B*, 1998, **45**, 144-149.
57 H. Fidder, J. Knoester and D. A. Wiersma, *J. Chem. Phys.*, 1991, **95**, 7880-7890.

TOC Graphic

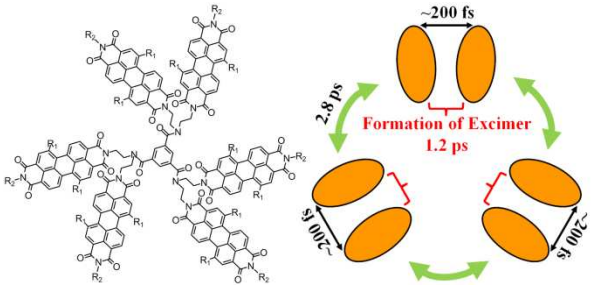

Two different interactions in PDI-hexamer: strong interaction in face-to-face dimer, and weak interaction among the separated dimers, are investigated.